



Mapping and monitoring of mangrove species in Eastern Lagoon National Park, Abu Dhabi, using Landsat 8 OLI data

Imen Ben Salem¹ · Yousef Nazzal¹ · Manish Sharma^{1,2} · Fares M. Howari³ · P. R. Kumaresan⁴ · Annamalai Karthi⁵ · Ahmed A. Al-Taani¹ · Lina Maloukh¹ · Cijo Xavier⁶

Received: 26 June 2023 / Accepted: 1 March 2024 / Published online: 11 March 2024
© Saudi Society for Geosciences and Springer Nature Switzerland AG 2024

Abstract

Mangrove species are shrubs and trees that are ecologically efficient and salt tolerant, predominantly grow in the intertidal region where land and ocean meet. These protects the shoreline from erosion, natural calamities, and climate change. Mapping, monitoring, and assessment of mangrove species are important for the conservation, restoration, and protection purposes. Earth observation using remote sensing satellite data plays a vital role in mapping and monitoring land-surface features. Studying mangroves with remote sensing also helps to track seasonal changes and understand how these ecosystems work. In the present study Mangrove species in and around Eastern Lagoon National Park of Abu Dhabi, United Arab Emirates, is mapped using the Multispectral Landsat 8 OLI data. It has been found that a large part of the area is covered by grey mangroves (i.e., *Avicennia marina*), including salt marshes. Vegetation indices like RVI, NDVI, SAVI, AVI, and CMRI are derived for mapping and health assessment to categorize mangrove species in high, medium, and low phenology activity, and found the maximum productivity was attained during March 2020 (0 to 366 days). Multispectral reflectance spectra of homogenous units were also collected and classified. For the first time, the satellite-based phenological information has been derived in the region using Landsat 8 OLI data, which will help in understanding biodiversity, climate change impacts, and human activities, and enabling decision-makers for the protection and sustainable use of these valuable coastal ecosystems.

Keywords Mangroves · Landsat 8 OLI · Phenology · Health assessment · Abu Dhabi · United Arab Emirates

Responsible Editor: Biswajeet Pradhan

✉ Manish Sharma
Manish.sharma@zu.ac.ae

Imen Ben Salem
Imen.BenSalem@zu.ac.ae

Yousef Nazzal
Yousef.nazzal@zu.ac.ae

Fares M. Howari
Fares.Howari@fvsu.edu

P. R. Kumaresan
kumaresanmoongis@gmail.com

Annamalai Karthi
karthiatkj@gmail.com

Ahmed A. Al-Taani
Ahmed.Al-Taani@zu.ac.ae

Lina Maloukh
Lina.Maloukh@zu.ac.ae

Cijo Xavier
cijo.xavier@newcastle.ac.uk

- 1 College of Natural and Health Sciences, Zayed University, Abu Dhabi, P.O. 144534, UAE
- 2 School of Earth, Atmosphere & Environment, Monash University, Victoria, Australia
- 3 College of Arts and Sciences, Fort Valley State University, Fort Valley, GA 31030-4313, USA
- 4 Civil Engineering Department, SRM Institute of Science and Technology, Chennai, Tamil Nadu, India
- 5 Centre for Applied Geology, The Gandhigram Rural Institute – Deemed to be University, Gandhigram, Dindigul, Tamil Nadu, India
- 6 SAgE Technical Services, Newcastle University, Newcastle upon Tyne, UK

Introduction

A mangrove forest acts as an interface between land and aquatic marine ecosystems. Mangrove trees have special traits that help them grow in salty and low-oxygen places (Giri et al. 2011; Duke et al. 2014; Tran et al. 2022; Simard et al. 2019; Kauffman et al. 2020). The assemblage of these kind of forest in the coastal environment helps in rapid sediment accretion, protection to the coastal zone, high carbon sequestration, and they also act as the biggest pool of carbon storage etc. (Alongi 2018). The coastal zones are fragile and prone to dynamic changes and natural calamities such as sea level rise, storm surges, Tsunami, etc. (Switzer et al. 2014), where the mangrove forest acts as a barrier and minimizes the disaster effects and reduces the impacts of climate extremities.

The intertidal zone of tropical and subtropical coastlines is often dominated by mangrove forests, which are extremely productive ecosystems. Monitoring of mangrove forest through remote sensing (RS) dates all the way back to 1960 (Wang et al. 2019; Pham et al. 2019; Maurya et al. 2021; Cardenas et al. 2017; Thakur et al. 2020). Hot themes in the field of mangrove RS have changed over the last 60 years, moving from the mapping of mangrove distribution to the inversion of biophysical parameters to the characterization of ecological processes (Wang et al. 2019; Pastor-Guzman et al. 2018). Some of the significant research studies were described based on the literature reviews of the mangroves across the world based on the remote sensing data. To assess the Matang Mangrove Forest Reserve in the northern region of Peninsular Malaysia, Rhyma et al. (2020) utilized Satellite Pour observation de la Terre (SPOT) satellite imagery captured on January 29 and July 9, 2016. They established a correlation between the Normalized Difference Vegetation Index (NDVI) and Soil-Adjusted Vegetation Index (SAVI) values extracted from the satellite images and field sample sites within the Matang Mangrove Forest Reserve.

Zhang et al. (2017) had mapped the mangrove forest in the coast of Fangcheng gang city, China, and surrounding land surface features using Landsat 8 OLI data. In that study, the decision-tree-based procedures were followed for mapping the mangrove species from other landforms with NDVI and Normalized Difference Moisture Index (NDMI) vegetation indices, which shown the better accuracy in mapping mangrove forests than traditional methods. Pastor-Guzman et al. (2018) conducted a study to determine the phenological parameters of mangrove forests in southeast Mexico's Yucatan Peninsula and identify the environmental factors influencing the phenological characteristics of these mangrove species. To assess the phenological status of the mangrove forests,

the researchers employed various techniques, including the analysis of vegetation indices such as the Normalized Difference Vegetation Index (NDVI), Enhanced Vegetation Index (EVI), Green Normalized Vegetation Index (gNDVI), and Normalized Difference Water Index (NDWI) using time-series data from the Moderate Resolution Imaging Spectroradiometer (MODIS) with a spatial resolution of 1 km. Phenological measures were derived by analyzing correlational data obtained from field samples. The study's results indicate that the mangrove species in the Yucatan Peninsula exhibit rapid growth, primarily influenced by rainfall patterns.

Son et al. (2016) investigated the spatiotemporal changes of mangrove forest in Can Gio Biosphere Reserve, Vietnam, from 1986 to 2014 using the Landsat series datasets. Additionally, the Google Earth images were also utilized for ground referencing of classified images. The tasseled cap transformation was performed to delineate mangrove from other land surface features. Previous literatures assessed the accuracy of resultant images, available land uses, land cover maps, and Google Earth imagery. Akbar et al. (2020) have incorporated Sentinel-2 Level 1 data from 2017 to 2020 by gathering monthly representative data every year in Segara Anakan, Cilacap District and implementing NDVI method to analyze the mangroves' health. Eventually, the results from the satellite images show that mangroves in Segara Anakan are experiencing a negative trend regarding their health from year to year. De Jong et al. (2021) have mapped the mangrove ecosystem and colonization patterns of Suriname situated in the Guiana coastline using Landsat series data. The changes in mangrove species and surrounding landforms were classified based on NDVI values. Intensive analysis of NDVI resulted in the gain and loss of mangrove species. The areas' growth rate (Re-habitation) was assessed for their long-term monitoring and restoration.

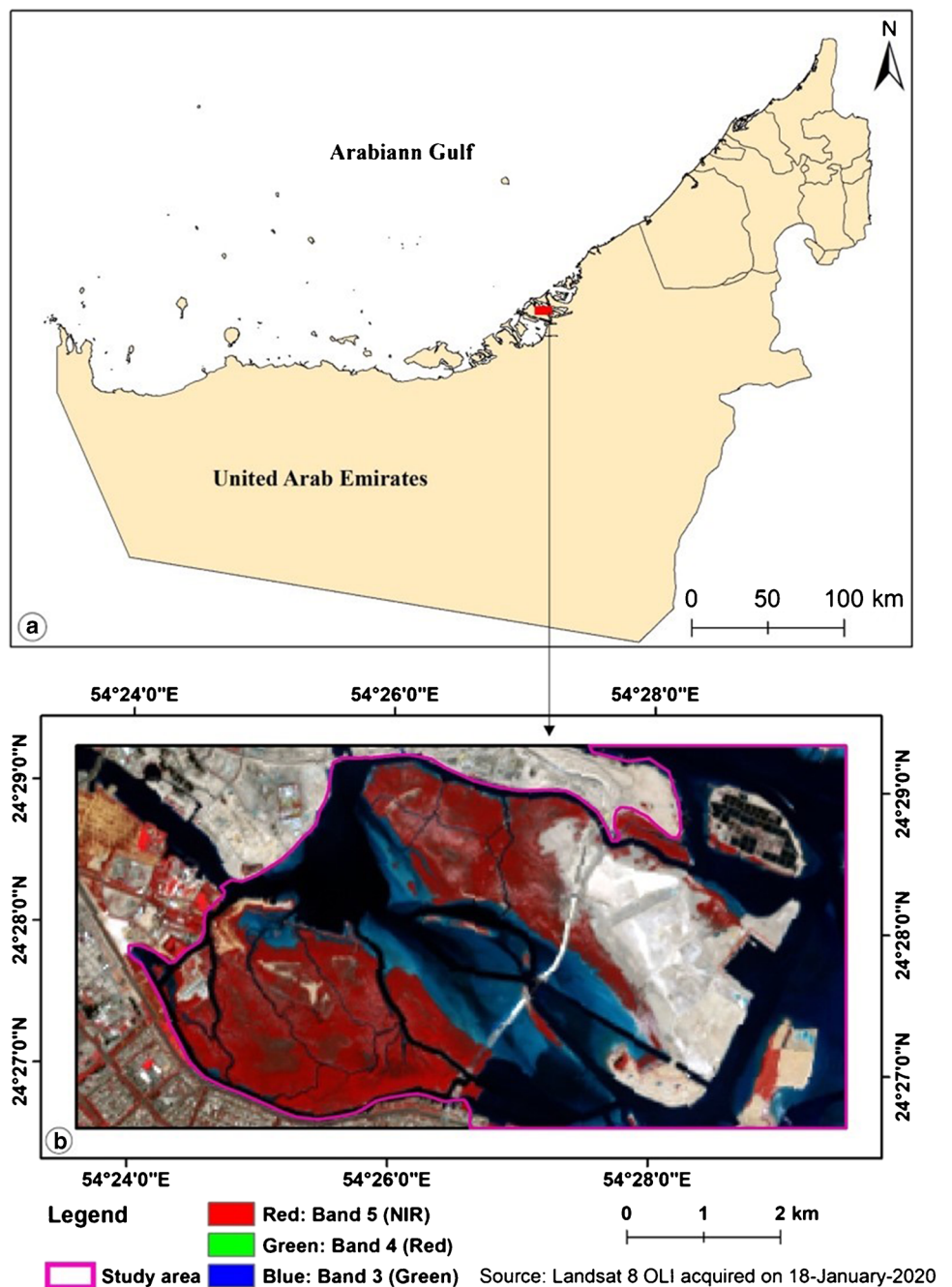
With above listed previous studies concerns, the present research holds significant value to map the Mangrove species in Eastern Lagoon National Park of Abu Dhabi Emirate by extensively utilizing Landsat 8 Operational Land Imager (OLI) multispectral data with a spatial resolution of 30m. Studying mangroves in the UAE provides a valuable case study for researchers worldwide. The extreme environmental conditions, including high salinity and arid climate, make UAE mangroves an interesting model for adaptation and resilience studies. Moreover, mangroves serve as natural carbon sinks, and comprehensive research contributes to global climate change mitigation efforts. In the UAE's context, current research aligns with the nation's commitment to environmental conservation, supporting their ambitious goals for mangrove plantation. It also allows for a deeper understanding of these critical ecosystems and their response to environmental changes. This research provides essential data for

assessing the health and dynamics of mangroves, helping researchers and policymakers make informed decisions. It also supports the development of innovative conservation and restoration strategies. Furthermore, the UAE’s efforts in mangrove plantation for coastal protection and biodiversity enhancement provide a unique opportunity for research on restoration techniques and their ecological impacts.

Study area

The mangroves in and around the Eastern Lagoon National Park of Abu Dhabi Emirate are taken for investigation, as shown in Fig. 1. The study area is characterized by hot arid climatic conditions (desert), high saline seawater of coastal environment, nearly flat topography, and several interconnected tidal creeks. The UAE has a coastline of 1318 km, with more than 80 km² of mangroves on its shore (Almahasheer 2018). These regions are fragile

Fig. 1 a The keymap represents the location of the study area, b the color composite map shows mangrove species in Eastern Mangrove Lagoon National Park and surrounding in Abu Dhabi, UAE (reddish color)



environments and prone to threat. Systematic and periodical monitoring is needed to preserve and conserve these fragile mangrove ecosystems. The periodic Landsat data archive provides the multispectral data in 30m spatial resolution with a temporal resolution of 16 days. Reflectance data can be subjected to various spectral indices, and vegetation parameter. Vegetation phenology is defined as the growing cycle of plants/trees across their growing seasons. The mangrove species are found in the lagoons and associated with the sheltered intertidal flats characterized by loose muddy to shady soils, not rising more than 2m above low tide level. The mangrove stand in the study site is inundated by tides twice daily (diurnal), with speeds not exceeding 0.5 knots (Embabi 1993). The main mangrove species in this region are the following:

- Grey mangroves - *Avicennia marina*
- Salt marshes - *Arthrocnemum macrostachyum*

The average height of the *Avicennia marina* species is about 3 m and can reach up to 7 m in some areas (Alsumaiti 2014). The climatic condition of the study region is divided in two seasons as summer (April to September) and winter (October to March). Monsoon (rainfall) occurs from November to February, with precipitation barely reaching 12 cm per year (Issa et al. 2019). According to Hegazy (1998), the

Arabian Gulf *Avicennia marina* is an evergreen species and usually has two phenological cycles:

1. Vegetative activity – maximum growth in March
2. Reproductive cycle (flower bud development) – flower budding starts in April, fruiting in May to August, and fruit maturation ends in September/October. Minimum growth in late autumn and early winter.

The biological lifecycle involves sequences of leaf unfolding and development, flowering, leaf senescence, and litterfall. These phenological changes can be mapped using satellite remote sensing data sets (Henebry et al. 2005; Friedl et al. 2006; Reed et al. 2009; Kimball 2014), which also needs to analyze with respect to climatic conditions.

Data collection and processing techniques

Methodology, data collection, and its specifications

Landsat 8 OLI multispectral datasets having cloud coverage less than 10% were collected from the Earth Explorer website (<http://earthexplorer.usgs.gov/>). to map and assess mangrove species. It is having 11 bands in the electromagnetic spectrum varying from visible, near infrared, short-wave, to thermal infrared regions. The specifications of used Landsat 8 OLI bands are described in Table 1. We focused

Table 1 Specifications of Landsat 8 OLI

Spectrum range	Band no.	Wavelength (µm)	Band center (µm)	Band center (nm)	Remarks	Spatial resolution
Visible	1	0.43–0.451	0.443	443	Coastal aerosol	30
	2	0.452–0.512	0.482	482	Blue	30
	3	0.533–0.590	0.5615	561.5	Green	30
	4	0.636–0.673	0.6545	654.5	Red	30
Near infrared	5	0.851–0.879	0.865	865	NIR	30
Short wave infra-red	6	1.566–1.651	1.6085	1608.5	SWIR1	30
	7	2.107–2.294	2.2005	2200.5	SWIR2	30

Table 2 Collected Landsat 8 OLI data and detail specifications

S. no.	Landsat 8 OLI data ID	Landsat 8 OLI data collected date	Path and row	No. of days in the year [2020] (0–366 days)	Sun elevation angle
1	LC08_L1TP_161043_20200118_20200823_02_T1	18-January-2020	161 and 43	18	38.3890
2	LC08_L1TP_160043_20200331_20200822_02_T1	30-March-2020	160 and 43	90	59.1485
3	LC08_L1TP_160043_20200518_20200820_02_T1	18-May-2020	160 and 43	140	68.7066
4	LC08_L1TP_160043_20200705_20200913_02_T1	05-July-2020	160 and 43	187	67.6419
5	LC08_L1TP_160043_20200923_20201006_02_T1	23-Sept.-2020	160 and 43	267	57.8095
6	LC08_L1TP_160043_20201228_20210310_02_T1	28-Dec.-2020	160 and 43	362	37.0423

for the year of 2020, and the collected datasets information for processing and analysis is shown in Table 2, with sun elevation angle.

Data processing techniques

Landsat 8 OLI Collection 2 Level 1 products are radiometrically and geometrically corrected image data for each spectral band, represented as calibrated and quantized scaled digital numbers (DN). The DN is commonly used to describe pixel values not yet converted into physically meaningful units (e.g., top-of-atmosphere (TOA) radiance or reflectance), which is the first step for using any remotely sensed data in quantitative investigations, through a process known as absolute radiometric calibration (Teixeira Pinto et al. 2020). In the first step, the DN values are converted into meaningful reflectance values using the formula mentioned below (Ihlen 2019).

$$\rho\lambda' = (M_\rho \times Q_{cal} + A_\rho) / \text{Sin}(\theta_{SE})$$

where $\rho\lambda'$ = top of atmosphere planetary reflectance, M_ρ = band-specific multiplicative rescaling factor, Q_{cal} = quantized and calibrated standard product pixel values or DN, A_ρ = band-specific additive rescaling factor, θ_{SE} = sun elevation angle of respective data.

The land-based phenological studies of grey mangroves in the Arabian Gulf indicate that maximum vegetation activity is attained during March (Hegazy 1998). The Landsat data for March month has been used for the multispectral diversity mapping and reflectance spectra analysis. The reflectance spectra/ endmembers from the study region were collected using ENVI software Sequential Maximum Angle Convex Cone (SMACC) module, which provides spectral endmembers (Gruninger et al. 2004). These endmembers are reflectance spectra composed of homogenous surface materials and pure in composition. The collected endmembers were given as input for classification, and the

result classified output image was derived using an optimum threshold. Spectral Angle Mapper is one of the classification techniques performed based on the physical characteristics of the spectra. The classification is performed based on the n-dimensional angle to match the input and pixel spectra of the image (Kruse et al. 1993). The vegetation indices were derived using calibrated Landsat reflectance data. Vegetation information from remotely sensed images are mainly analyzed and interpreted by band rationing techniques to assess the differences and changes of the green leaves from species and canopy spectral characteristics. The vegetation indices give quantitative information regarding the vigor of vegetation in the particular region (Campbell 1987), which exhibits better sensitivity in detecting above-ground biomass, and then utilization of individual spectral bands for interpretation (Asrar et al. 1984; Bannari et al. 1995). The vegetation indices used in this study are shown in Table 3 with formulations used.

The NDVI is used in the current study as it indicates the vigor and greenness of the species, which resulted in analysis and detection of phenological variation during the year 2020. The other vegetation indices have been used for the health assessment of mangrove species. The overall methodology followed in this research is shown as a flowchart in Fig. 2.

Results

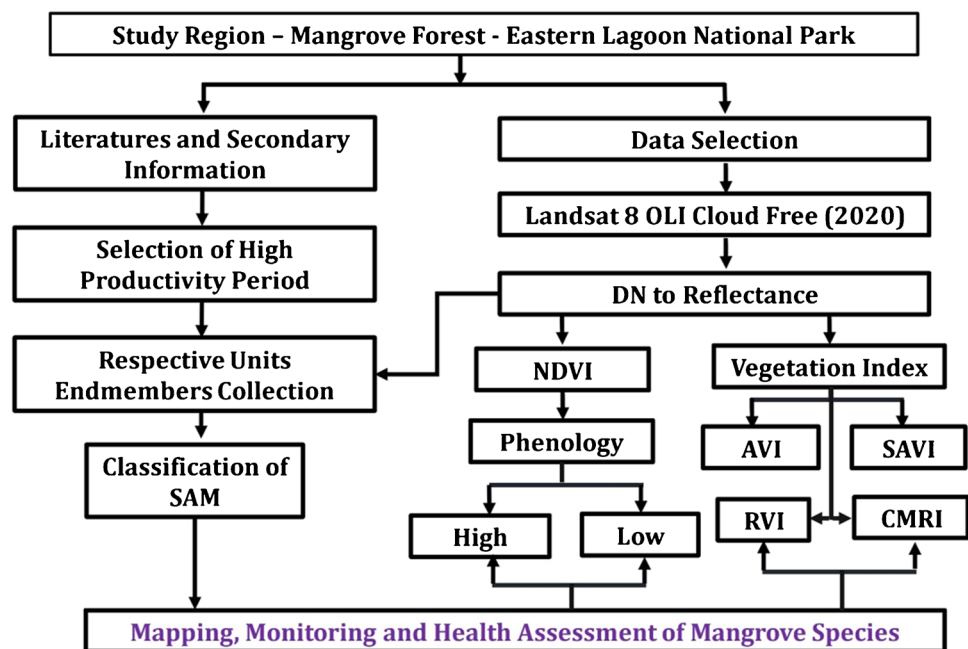
Collection of multispectral reflectance spectra and classification

The mangroves in and around Eastern Lagoon National Park of Abu Dhabi are enriched with *Avicennia marina* (grey mangroves), and *Arthrocnemum macrostachyum* (Salt Marshes) (Almahasheer 2018; Saito et al. 2003; Habshi et al. 2007; Elmahdy and Mohamed 2013; Moore et al. 2015; Samara et al. 2020; Mateos-Molina et al. 2020). The

Table 3 Vegetation indices with proposed authors and their formula

S. no.	Index name	Acronym	Author with year	Formula	ENVI band math formula
1.	RVI	Ratio Vegetation Index	Jordan 1969	NIR / RED	B5 / B4
2.	NDVI	Normalized Difference Vegetation Index	Rouse et al. 1974	$(NIR - RED) / (NIR + RED)$	$B5 - B4 / B5 + B4$
3.	AVI	Advanced Vegetation Index	Roy et al. 1996	$[NIR \times (1 - RED) \times (NIR - RED)]^{1/3}$	$[B5 \times (1 - B4) \times (B5 - B4)]^{1/3}$
4.	SAVI	Soil-Adjusted Vegetation Index	Huete 1988	$(NIR - RED / NIR + RED + 0.5) \times (1 + 0.5)$ *L=0.5 (constant)	$(B5 - B4 / B5 + B4 + 0.5) \times (1 + 0.5)$
5.	CMRI	Combined Mangrove Recognition Index	Gupta et al. 2018	$(NIR - RED / NIR + RED) - (GREEN - RED / GREEN + RED)$	$(B5 - B4 / B5 + B4) - (B3 - B4 / B3 + B4)$

Fig. 2 The proposed methodology is adopted in the present study



Avicennia marina is evergreen mangrove species. It shows vegetation activity throughout the year (0-365/366 days), and maximum growth activity is found in March. The maximum growth is attained before the flower bud development period. Accordingly, the availability of data collection for the March month (30/03/2020) data has been chosen for multispectral diversity mapping. SMACC module is used to collect the endmembers as shown in Fig. 3a. The density variation plays a major role in the spectral diversity of the region. The four distinct homogenous units were identified: Dense, Sparse, and Open *Avicennia marina* and *Arthrocnemum macrostachyum*.

All four species observed to have a high value in the NIR range, whereas value varies in red band (depending on their nature) and in SWIR range, the reflectance value seems to drop. Four endmembers were collected and given as input to classify the scene. For classification, an optimum threshold of 0.1 was used in the SAM-based classification. The Dense *Avicennia Marina* covers 2.287 km², Open *Avicennia Marina* covers 3.910 km², Sparse *Avicennia Marina* covers 2.072 km² and *Arthrocnemum macrostachyum* covers 1.131 km² area.

NDVI and phenology variation of mangrove species

NDVI is calculated based on the utilization of NIR (0.851–0.879) and Red (0.636–0.673) bands of the Landsat 8 OLI image. NDVI is a direct indication of vegetation vigor and state of the region. The normalization process of Red and NIR bands allows them in global usage for descriptor of vegetation variations despite its atmospheric effects and sensor calibration degradation (Bannari et al. 1995; Kaufman

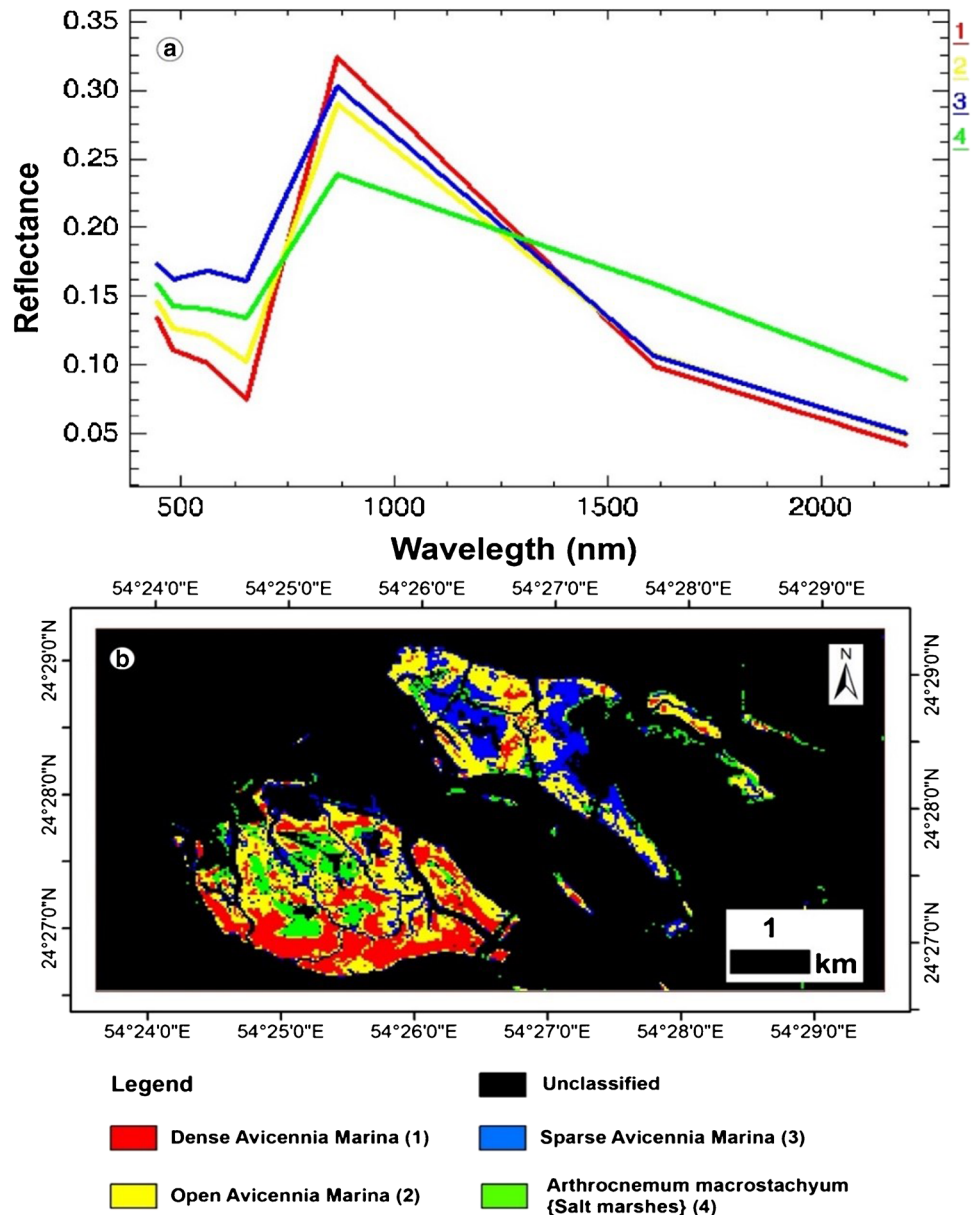
1984; Fraser and Kaufman 1985; Prince and Tucker 1986; Townshend and Justice 1986; Deblonde and Cihlar 1993; Holben et al. 1990). The NDVI value ranges between -1 to $+1$, and a higher value indicates dense vegetation, whereas low value shows sparse vegetation. The temporal datasets collected (18th, 90th, 140th, 187th, 267th and 362nd day of year 2020) are utilized for the generation of NDVI map. The resultant NDVI images are shown in Fig. 4, in the order of 0 to 365/366 days accordingly.

Phenology is referred to the life cycle of vegetation processes. The phenological events have been categorized based on the vegetation periods such as maximum leaf appearances, leaf fall, flowering, and fruiting (Duke 1990). The phenology can be mapped and monitored using remote sensing techniques without damaging/harming the Earth observational satellites (Pastor-Guzman et al. 2018; Schwartz 2003; Reed et al. 2009; Klostermann et al. 2014; Adole et al. 2016; Rani et al. 2016). In this study, the high and low phenological activity periods were also identified through the results of NDVI values of the 2020-year Landsat 8 OLI data (Fig. 5).

To assess the health of the mangroves, Landsat 8 OLI data of March month is compared with July. Several vegetation indices were applied to observe the high and lowest phenological activity period as shown in Table 3. To discriminate the non-mangroves and mangroves in the vegetation indices, the optimum threshold was estimated. The health assessment of mangroves was observed by categorizing the vegetation indices values into high, medium, and low, as shown in Fig. 6.

The Ratio Vegetation Index (RVI) is generated based on a simple ratio using NIR and RED bands (Jordan 1969),

Fig. 3 **a** The collected endmember spectra using Landsat 8 OLI data for 30th March 2020; **b** Spectral Angle Mapper (SAM) classified image with a threshold of 0.1, showing mangrove species highlighted in different color units



showing values ranging between 0 and 10, showing the sensitivity to the atmospheric effects and ground optical properties (High for vegetation, low for soil, ice, water, etc.) (Ban-nari et al. 1995; Baret and Guyot 1991). The RVI of March and July month is shown in Fig. 6(a) and (b). It discriminates the mangrove species from other landforms. Several authors used this to extract and classify particular interest such as vegetation by using optimum threshold (Otsu 1979). In the current study, the resultant RVI image is classified with an optimum threshold of 1.3. Furthermore, the classification was done with reaming values into high (2.51 and above), medium (1.51–2.5), and low (1.31–1.5).

The Advanced Vegetation Index (AVI) is mapped using the NIR and RED bands with power values (Roy et al. 1996). The AVI is sensitive to vegetation species’ density

and canopy coverage (Roy et al. 1996; Qi et al. 2013; Su Mon et al. 2012; Himayah and Danoedoro 2016). The March data exhibits high densities and maximum vigor, whereas the July data indicates a lower density value. The region rich in salt marshes had also shown poor AVI values. The optimum threshold of 0.008 is used to discriminate the mangrove species from other landforms. The AVI resultant image is further classified into high (0.21 and above), medium (0.051 – 0.02), low (0.0081 – 0.015) as shown in Fig. 6(c) and (d).

The Soil-Adjusted Vegetation Index (SAVI) is similar to NDVI but uses the soil-brightness correction factor (0 to 1) to minimize the soil brightness effects in the vegetation index (Huete 1988). The optimum threshold of 0.1 is used to discriminate the mangrove from other landforms. The classification of SAVI is done by giving high (0.31 and above),

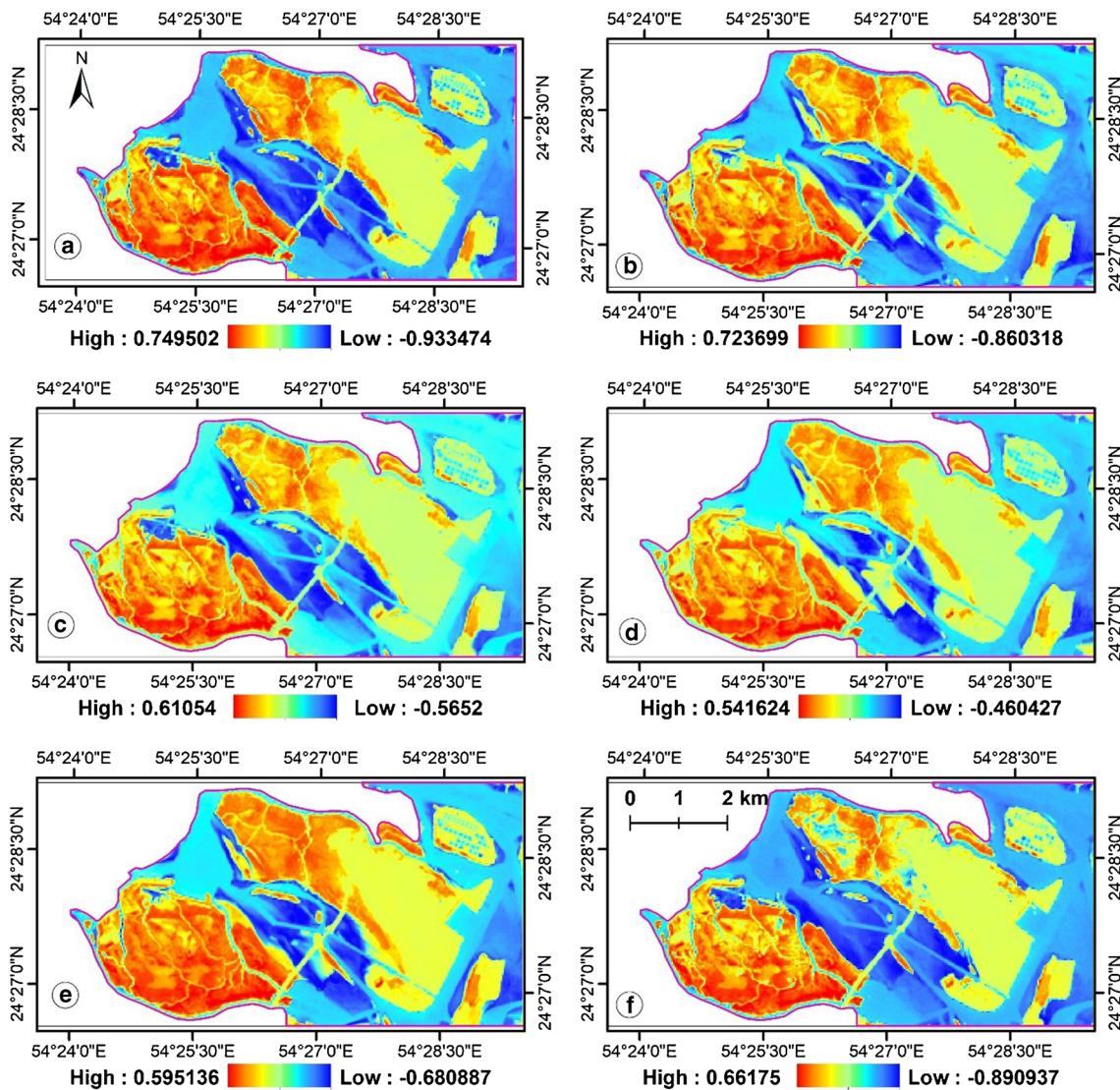


Fig. 4 Normalized Difference Vegetation Index (NDVI) resultant images of **a** 18th, **b** 90th, **c** 140th, **d** 187th, **e** 267th, and **f** 362nd days of the year 2020. Red color indicates densely vegetated and blue color denotes sparsely vegetated region

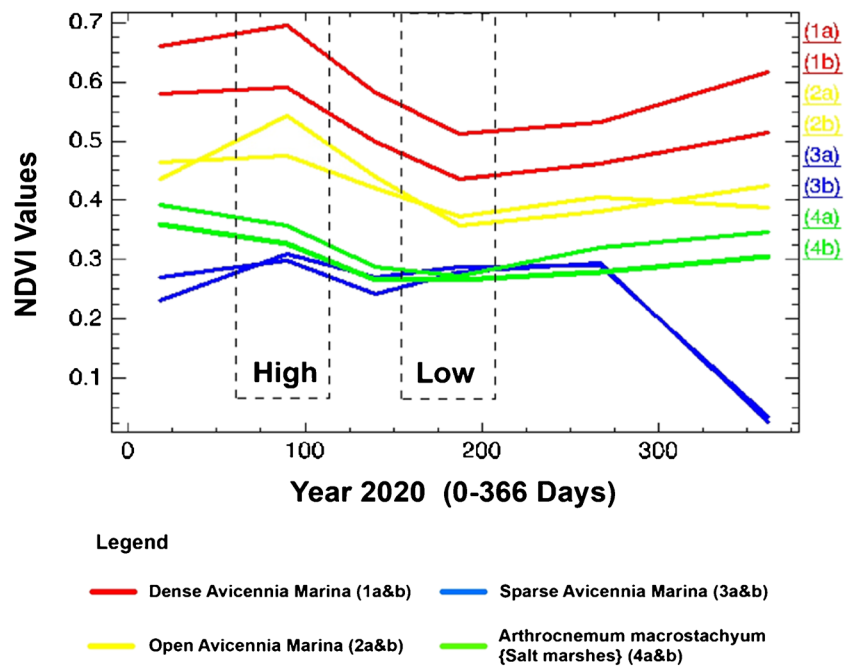
medium (0.21–0.3), and low (0.11–0.2) values as shown in Fig. 6(e) and (f). SAVI helps to delineate the mangrove species more precisely from other landforms and also its variations within the mangroves. The Combined Mangrove Recognition Index (CMRI) uses the band ratio technique by utilizing the NIR, RED, and GREEN reflectance bands. The accuracy and water absorption are exploited by including the green band in the index (Gupta et al. 2018). The optimum threshold used in CMRI to discriminate the mangrove species from other landforms is 0.2.

The CMRI output was classified by giving high (0.41 and above), medium (0.31–0.4), and low (0.21–0.3) values as shown in Fig. 6(g) and (h). This index also performs well with discriminating variations within mangroves concerning chlorophyll content, density, and canopy cover.

Satellite-derived mangrove phenology and rainfall

Rainfall plays a vital role in the growth of mangrove species, and it gives freshwater to the coastal and hypersaline environment. It also triggers the dispersal of seedlings and favors the condition by lowering salinity (Lopez-Portillo and Ezcurra 1985). In the current study, the hydrological season starts from 1st September to and ends on 31st August. The rainfall plays a major role in the growth of the *Avicennia marina* (grey mangroves). Ouarda et al. (2014) have analyzed rainfall data of the Arabian Gulf and found that the rainfall increases in November and attains peak in March, whereas in May, it starts to decline and lowers at the end of August (Ouarda et al. 2014; Niranjan Kumar and Ouarda 2014). The precipitation from December to March affects

Fig. 5 Remote sensing-based phenological study during the year 2020 (0–366) of mangrove species in and around Eastern Lagoon National Park of Abu Dhabi



the high phenological growth during march month vegetation indices derived from the 2020-year Landsat 8 OLI data analysis.

Discussion

Mangroves are incredible ecosystems that thrive in coastal regions. In Abu Dhabi, these unique habitats play a crucial role in maintaining biodiversity, protecting shorelines, and mitigating climate change impacts. With the UAE's national priority to plant millions of mangroves, it becomes paramount to also prioritize the understanding of the nature and properties of previously planted mangroves. The collection and classification of multispectral reflectance spectra of homogeneous units played a crucial role in mapping and understanding the distribution of type of mangroves and other vegetation types in the study area. Landsat data captured a range of information, including reflectance at different wavelengths, which helped to discriminate between different mangrove species. By examining the unique spectral signatures of various vegetation types, it becomes possible to distinguish between *Avicennia marina*, salt marshes, and other coastal vegetation. This classification provides valuable insights into the distribution, health etc.

The mangroves in and around Eastern Lagoon National Park of Abu Dhabi are enriched with *Avicennia marina*, and *Arthrocnemum macrostachyum*. SMACC module and SAM classification with an optimal threshold of 0.1 have revealed the 2.287 km² of aerial coverage for Dense *Avicennia Marina*, 3.910 km² for Open *Avicennia Marina*,

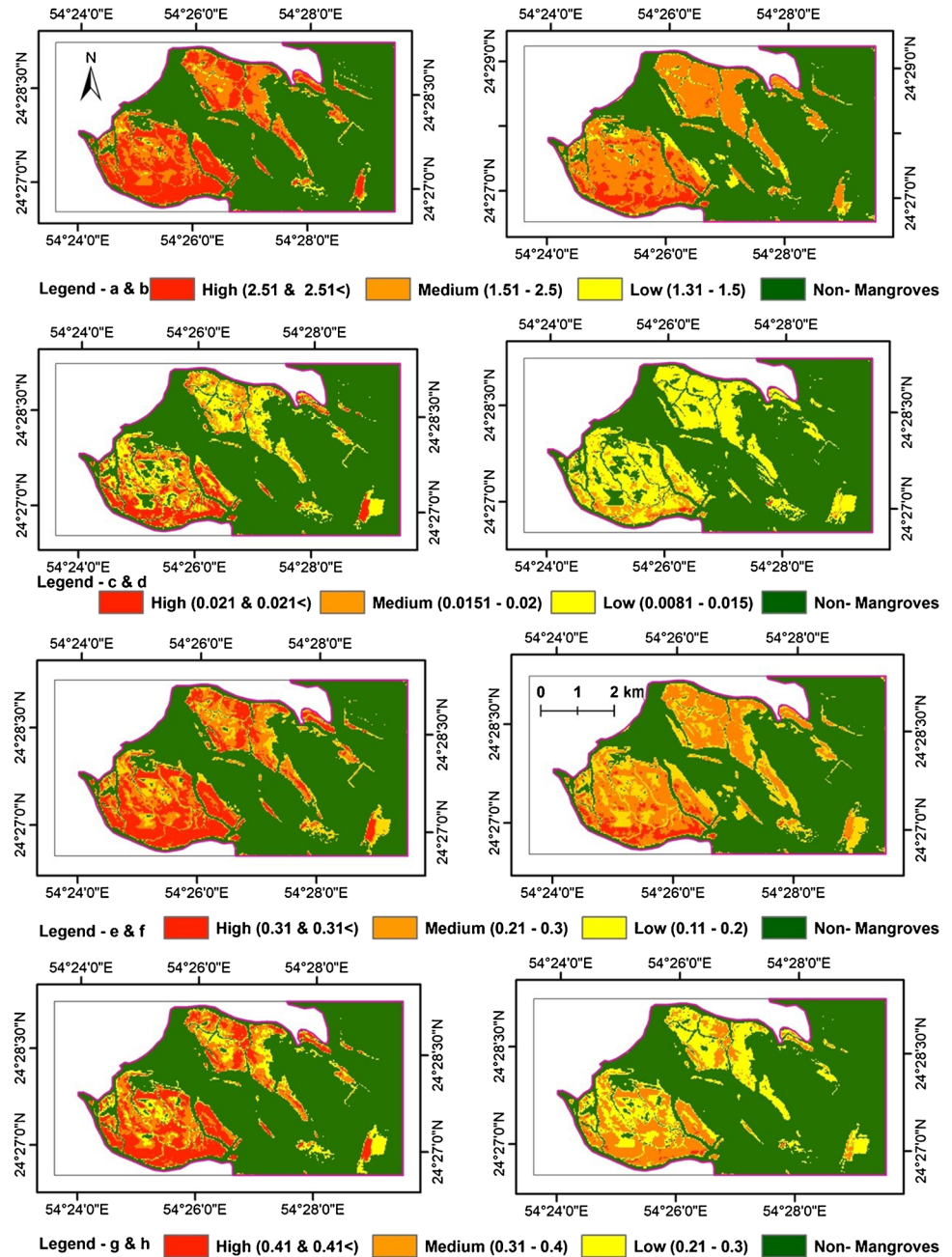
2.072 km² for Sparse *Avicennia Marina*, and 1.131 km² for *Arthrocnemum macrostachyum*.

Avicennia marina, a species of mangrove tree found in Abu Dhabi, exhibits remarkable adaptations that enable it to thrive in the challenging conditions of intertidal areas, where water levels fluctuate, and salinity levels are high. One of its distinctive features is the development of specialized aerial roots called pneumatophores, which are common and essential in mangrove ecosystems. These pneumatophores serve a dual purpose by allowing the tree to absorb oxygen from the air and excrete excess salt, giving it a unique advantage in these harsh environments (Srikanth et al. 2016). This ability to endure such conditions is further supported by the availability of sediment rich in organic matter and nutrients, along with the regular tidal inundation, creating a fertile habitat for *Avicennia marina* to grow and flourish.

In addition to its survival strategies, mangroves like *Avicennia marina* often exist in proximity to salt marshes, which serve as valuable ecosystems. These salt marshes play a critical role in trapping sediments, reducing wave energy, and providing additional shelter and food resources for a variety of species. The sturdy root systems of grey mangroves, such as *Avicennia marina*, contribute to the stabilization of coastlines, underscoring their ecological significance in maintaining the delicate balance of intertidal environments.

In Abu Dhabi, the climate follows a distinct pattern of wet and dry seasons. March marks the beginning of warmer and wetter weather after a period of cooler and drier conditions. This shift in climate has a noticeable impact on grey mangroves, leading to increased growth, which can observe with the emergence of new buds,

Fig. 6 Health assessment based on vegetation indices of March month **a** Ratio Vegetation Index, **c** Advanced Vegetation Index, **e** Soil-Adjusted Vegetation Index, and **g** Combined Mangrove Recognition Index; health assessment based on vegetation indices of July month (b) Ratio Vegetation Index, (d) Advanced Vegetation Index, (f) Soil-Adjusted Vegetation Index, and (h) Combined Mangrove Recognition Index



leaves, and a greener appearance. The peak of this growth, known as phenological activity, observed in March, while it decreases significantly in July when the weather is drier and hotter.

Tidal activity, particularly high tides, affects mangrove species close to the coast. During high tide periods like December, parts of the mangroves get inundated by rising water. This impact on the mangroves is reflected in the phenological activity of Sparse *Avicennia Marina*, which shows lower values during December. These observations highlight the tidal patterns impacting the behavior of mangroves in this region.

The peak productivity observed in March 2020, as also indicated by various vegetation indices such as the Ratio Vegetation Index (RVI), Normalized Difference Vegetation Index (NDVI), Soil-Adjusted Vegetation Index (SAVI), Advanced Vegetation Index (AVI), and Combined Mangrove Recognition Index (CMRI), can be attributed to several interconnected factors. First, the timing of this peak productivity aligns with the climate and environmental conditions of Abu Dhabi during this period. March typically marks the transition from winter to spring, characterized by milder temperatures and increased sunlight. These favorable conditions stimulate photosynthesis and growth in vegetation.

Avicennia marina and other coastal plants exhibit a surge in photosynthetic activity during this period, contributing to enhanced vegetation indices.

Additionally, the high productivity observed in March 2020 is also linked with the environmental drivers such as precipitation, temperature, and the availability of water resources. Increased moisture from winter rains can provide ample water for plant growth, while the rising temperatures stimulate metabolic processes, boosting photosynthetic activity.

The remarkable ability of *Avicennia marina* to endure such extreme conditions makes it a crucial species for various ecological purposes. Its presence helps protect coastlines from erosion, as the intricate root system stabilizes the soil and prevents it from being washed away by tides and waves. Overall, *Avicennia marina* plays a vital role in preserving the delicate balance of intertidal environments and supporting the biodiversity that relies on them.

Conclusions

The mapping and monitoring of mangrove species and their phenology are crucial in the accurate and sustainable management of forests and shorelines. The mangroves forest is a fragile environment subjected to threat all over the world. The Landsat 8 OLI bands are very useful in mapping, monitoring, and classifying mangrove species with their optimum spatial and spectral capability. Even though hyperspectral remote sensing satellite data can give better results, but data availability is comparatively less and cost-effective.

For the first time, the satellite-based phenological information has been derived from the year 2020 using Landsat 8 OLI data. Our results indicate that March month gives high vegetation activity for mangrove species in Abu Dhabi coastal region. Abu Dhabi is mainly dominated by *Avicennia marina* (grey mangroves). Remote sensing-based multispectral vegetation indices such as SAVI, AVI, and CMRI are delineated, and health assessment of mangrove species has been derived. Environmental drivers, i.e., rainfall, play a vital role in the growth of Mangrove species, and is the main source of fresh water in extreme climatic conditions like Abu Dhabi. From the historical evolution of earth observation, satellite imageries give tremendous inputs in understanding the earth phenomenon. Future work of the current study is to explore the Mangrove Forest using hyperspectral remote sensing data.

Author contributions Conceptualization: I.B.S., M.S., and P.R.K.; methodology: I.B.S., M.S., and P.R.K.; software: M.S., P.R.K., and A.K.; validation: I.B.S., M.S., and F.H.; formal analysis: I.B.S., M.S., and P.R.K.; investigation: M.S., P.R.K., and A.K.; resources: M.S., K.A., P.R.K., and Y.N.; data curation: M.S., P.R.K., A.K., and C.M.X.; writing—original draft preparation: I.B.S., M.S., and P.R.K.;

writing—review and editing: M.S., I.B.S., and A.K.; visualization: I.B.S., M.S., P.R.K., A.A.T., L.M., and C.M.X.; supervision: I.B.S.; funding acquisition: I.B.S.

Funding This project was funded by the Research Office, Zayed University, United Arab Emirates (Project No. R 21005).

Data availability The raw data supporting the conclusions of this article will be made available by the authors, without undue reservation.

Declarations

Conflict of interest The authors declare no competing interests.

References

- Adole T, Dash J, Atkinson PM (2016) A systematic review of vegetation phenology in Africa. *Ecol Inform* 34:117–128
- Akbar MR, Arisanto PAA, Sukirno BA, Merdeka PH, Priadhi MM, Zallesa S (2020) Mangrove vegetation health index analysis by implementing NDVI (normalized difference vegetation index) classification method on sentinel-2 image data case study: Segara Anakan, Kabupaten Cilacap. *IOP Confer Ser Earth Environ Sci* 584(1):012069. <https://doi.org/10.1088/1755-1315/584/1/012069>
- Almhasheer H (2018) Spatial coverage of mangrove communities in the Arabian Gulf. *Environ Monit Assess* 190(2):85
- Alongi DM (2018) Mangrove Forests. In: *Blue Carbon*. Springer Briefs in Climate Studies. Springer, Cham, pp 23–36. https://doi.org/10.1007/978-3-319-91698-9_3
- Alsumaiti TS (2014) An assessment of *Avicennia marina* forest structure and aboveground biomass in Eastern Mangrove Lagoon National Park, Abu Dhabi. *Arab World Geogr* 17:166–185
- Asrar GQ, Fuchs M, Kanemasu ET, Hatfield JL (1984) Estimating absorbed photosynthetic radiation and leaf area index from spectral reflectance in wheat 1. *Agron J* 76:300–306. <https://doi.org/10.2134/agronj1984.00021962007600020029x>
- Bannari A, Morin D, Bonn F, Huete A (1995) A review of vegetation indices. *Remote Sens Rev* 1(13):95–120. <https://doi.org/10.1080/02757259509532298>
- Baret F, Guyot G (1991) Potentials and limits of vegetation indices for LAI and APAR assessment. *Remote Sens Environ* 35:161–173. [https://doi.org/10.1016/0034-4257\(91\)90009-U](https://doi.org/10.1016/0034-4257(91)90009-U)
- Campbell JB (1987) *Introduction to remote sensing*. The Guilford Press
- Cardenas NY, Joyce KE, Maier SW (2017) Monitoring mangrove forests: are we taking full advantage of technology? *Int J Appl Earth Obs Geoinf* 63:1–14
- De Jong SM, Shen Y, de Vries J, Bijnaar G, van Maanen B, Augustinus P, Verweij P (2021) Mapping mangrove dynamics and colonization patterns at the Suriname coast using historic satellite data and the LandTrendr algorithm. *Int J Appl Obs Geoinf* 97:102293. <https://doi.org/10.1016/j.jag.2020.102293>
- Deblonde G, Cihlar J (1993) A multiyear analysis of the relationship between surface environmental variables and NDVI over the Canadian landmass. *Remote Sens Rev* 7(2):151–177. <https://doi.org/10.1080/02757259309532172>
- Duke N, Nagelkerken I, Agardy T, Wells S, Van Lavieren H (2014) The importance of mangroves to people: a call to action. United Nations Environment Programme World Conservation Monitoring Centre, Cambridge, UK ISBN 92-807-3397-4
- Duke NC (1990) Phenological trends with latitude in the mangrove tree *Avicennia marina*. *J Ecol* 78(1):113–133. <https://doi.org/10.2307/2261040>

- Elmahdy SI, Mohamed MM (2013) Change detection and mapping of mangrove using multi-temporal remote sensing data: a case study of Abu Dhabi, UAE. *J Geom* 7(1):41–45
- Embabi NS (1993) Environmental aspects of geographical distribution of mangrove in the United Arab Emirates. In: Lieth H, Masoom AA (eds) *Towards the rational use of high salinity tolerant plants. Tasks for vegetation science*, vol 27. Springer. https://doi.org/10.1007/978-94-011-1858-3_5
- Fraser RS, Kaufman YJ (1985) The relative importance of aerosol scattering and absorption in remote sensing. *IEEE Trans Geosc Remote Sens* 5:625–633. <https://doi.org/10.1109/TGRS.1985.289380>
- Friedl M, Henebry G, Reed B, Huete A (2006) Land surface phenology: a community white paper requested by NASA. Tech Rep, Chicago. https://cce.nasa.gov/mtg2008_ab_presentations/Phenology_Friedl_whitepaper.pdf
- Giri C, Ochieng E, Tieszen LL, Zhu Z, Singh A, Loveland T, Masek J, Duke N (2011) Status and distribution of mangrove forests of the world using earth observation satellite data. *Glob Ecol Biogeogr* 20:154–159
- Gruninger JH, Ratkowski AJ, Hoke ML (2004) The sequential maximum angle convex cone (SMACC) endmember model. In algorithms and technologies for multispectral, hyperspectral, and ultraspectral imagery. *Int Soc Opt Photon* 5425:1–14. <https://doi.org/10.1117/12.543794>
- Gupta K, Mukhopadhyay A, Giri S, Chanda A, Majumdar SD, Samanta S, Mitra D, Samal RN, Pattnaik AK, Hazra S (2018) An index for discrimination of mangroves from non-mangroves using LANDSAT 8 OLI imagery. *MethodsX* 5:1129–1139. <https://doi.org/10.1016/j.mex.2018.09.011>
- Habshi AA, Youssef T, Aizpuru M, Blasco F (2007) New mangrove ecosystem data along the UAE coast using remote sensing. *Aquat Ecosyst Health Manag* 10(3):309–319. <https://doi.org/10.1080/14634980701512525>
- Hegazy AK (1998) Perspectives on survival, phenology, litter fall and decomposition, and caloric content of *Avicennia marina* in the Arabian Gulf region. *J Arid Environ* 40:417–429. <https://doi.org/10.1006/jare.1998.0457>
- Henebry GM, de Beurs KM, Gitelson AA (2005) Land surface phenologies of Uzbekistan and Turkmenistan between 1982 and 1999. *Arid Ecosyst* 11:25–32
- Himayah S, Danodoro P (2016) The utilization of Landsat 8 multitemporal imagery and forest canopy density (FCD) model for forest reclamation priority of natural disaster areas at Kelud Mountain, East Java. *IOP Conf Ser Earth Environ Sci* 47(1):012043. <https://doi.org/10.1088/1755-1315/47/1/012043>
- Holben BN, Kaufman YJ, Kendall JD (1990) NOAA-11 AVHRR visible and near-IR inflight calibration. *Int J Remote Sens* 11(8):1511–1519. <https://doi.org/10.1080/01431169008955109>
- Huete AR (1988) A soil-adjusted vegetation index (SAVI). *Remote Sens Environ* 25(3):295–309. [https://doi.org/10.1016/0034-4257\(88\)90106-X](https://doi.org/10.1016/0034-4257(88)90106-X)
- Ihlen V (2019) *Landsat 8 Data Users Handbook*. US Geological Survey, Sioux Falls, SD, USA
- Issa S, Dahy B, Saleous N, Ksiksi T (2019) Carbon stock assessment of date palm using remote sensing coupled with field-based measurements in Abu Dhabi (United Arab Emirates). *Int J Remote Sens* 40:7561–7580. <https://doi.org/10.1080/01431161.2019.1602795>
- Jordan CF (1969) Derivation of leaf-area index from quality of light on the forest floor. *Ecology* 4:663–666. <https://doi.org/10.2307/1936256>
- Kauffman JB, Adame M, Arifanti VB, Schile-Beers LM, Bernardino AF, Bhomia RK, Donato DC, Feller IC, Ferreira TO, del Carmen Jesus Garcia M (2020) Total ecosystem carbon stocks of mangroves across broad global environmental and physical gradients. *Ecol Monogr* 90:e01405
- Kaufman YJ (1984) Atmospheric effects on remote sensing of surface reflectance. In *Remote sensing: critical review of technology*. *Int Soc Opt Photon* 475:20–33. <https://doi.org/10.1117/12.966238>
- Kimball J (2014) Vegetation Phenology. In: Njoku EG (ed) *Encyclopedia of remote sensing*. *Encyclopedia of Earth Sciences Series*. https://doi.org/10.1007/978-0-387-36699-9_188
- Klostermann ST, Hufkens K, Gray JM, Melaas E, Sonnentag O, Lavine I, Mitchell L, Norman R, Friedl MA, Richardson AD (2014) Evaluating remote sensing of deciduous forest phenology at multiple spatial scales using PhenoCam imagery. *Biogeosciences* 11(16):4305–4320. <https://doi.org/10.5194/bg-11-4305-2014>
- Kruse FA, Lefkoff AB, Boardman JW, Heidebrecht KB, Shapiro AT, Barloon PJ, Goetz AF (1993) The spectrimage processing system (SIPS)—interactive visualization and analysis of imaging spectrometer data. *Remote Sens Environ* 44:145–163. [https://doi.org/10.1016/0034-4257\(93\)90013-N](https://doi.org/10.1016/0034-4257(93)90013-N)
- Lopez-Portillo J, Ezcurra E (1985) Litter fall of *Avicennia germinans* L. in a one-year cycle in a mudflat at the Laguna de Mecocan, Tabasco, Mexico. *Biotropica* 1:186–190. <https://doi.org/10.2307/2388215>
- Mateos-Molina D, Antonopoulou M, Baldwin R, Bejarano I, Burt JA, García-Charton JA, Al-Ghais SM, Walgamme J, Taylor OJ (2020) Applying an integrated approach to coastal marine habitat mapping in the north-western United Arab Emirates. *Mar Environ Res* 161:105095. <https://doi.org/10.1016/j.marenvres.2020.105095>
- Maurya K, Mahajan S, Chaube N (2021) Remote sensing techniques: mapping and monitoring of mangrove ecosystem—a review *Complex Intell. Syst* 7:2797–2818
- Moore GE, Grizzle RE, Ward KM, Alshihhi RM (2015) Distribution, pore-water chemistry, and stand characteristics of the mangroves of the United Arab Emirates. *J Coas Res* 31(4):957–963. <https://doi.org/10.2112/JCOASTRES-D-14-00142.1>
- Niranjan Kumar K, Ouarda TB (2014) Precipitation variability over UAE and global SST teleconnections. *J Geop Res Atmospheres* 119(17):10–313. <https://doi.org/10.1002/2014JD021724>
- Otsu N (1979) A threshold selection method from gray-level histograms. *IEEE Trans Syst Man Cybern* 9(1):62–66. <https://doi.org/10.1109/TSMC.1979.4310076>
- Ouarda TB, Charron C, Kumar KN, Marpu PR, Ghedira H, Molini A, Khayal I (2014) Evolution of the rainfall regime in the United Arab Emirates. *J Hydrol* 514:258–270. <https://doi.org/10.1016/j.jhydrol.2014.04.032>
- Pastor-Guzman J, Dash J, Atkinson PM (2018) Remote sensing of mangrove forest phenology and its environmental drivers. *Remote Sens Environ* 205:71–84. <https://doi.org/10.1016/j.rse.2017.11.009>
- Pham TD, Yokoya N, Bui DT, Yoshino K, Friess DA (2019) Remote sensing approaches for monitoring mangrove species, structure, and biomass: opportunities and challenges. *Remote Sens* 11:230
- Prince SD, Tucker CJ (1986) Satellite remote sensing of rangelands in Botswana II. NOAA AVHRR and herbaceous vegetation. *Int J Remote Sens* 7(11):1555–1570. <https://doi.org/10.1080/01431168608948953>
- Qi X, Wang K, Zhang C (2013) Effectiveness of ecological restoration projects in a karst region of southwest China assessed using vegetation succession mapping. *Ecol Eng* 54:245–253. <https://doi.org/10.1016/j.ecoleng.2013.01.002>
- Rani V, Sreelekshmi S, Preethy CM, BijoyNandan S (2016) Phenology and litterfall dynamics structuring Ecosystem productivity in a tropical mangrove stand on South West coast of India. *Reg Stud Mar Sci* 8:400–407. <https://doi.org/10.1016/j.rsma.2016.02.008>
- Reed DN, Anderson TM, Dempewolf J, Metzger K, Serneels S (2009) The spatial distribution of vegetation types in the Serengeti ecosystem: the influence of rainfall and topographic relief on vegetation patch characteristics. *J Biogeogr* 36(4):770–782. <https://doi.org/10.1111/j.1365-2699.2008.02017.x>

- Rhyma PP, Norizah K, Hamdan O, Faridah-Hanum I, Zulfa AW (2020) Integration of normalised different vegetation index and Soil-Adjusted Vegetation Index for mangrove vegetation delineation. *Remote Sens Appl: Soc Environ* 1(17):100280. <https://doi.org/10.1016/j.rsase.2019.100280>
- Rouse JW, Hass RH, Schell JA, Freden SC, Mercanti EP, Becker MA (1974) Monitoring vegetation system in the great palins with ERTS. *Third Earth Resource Technology Satellite-1. Symposium Technical presentation*, 309-317.
- Roy PS, Sharma KP, Jain A (1996) Stratification of density in dry deciduous forest using satellite remote sensing digital data—an approach based on spectral indices. *J Biosci* 21(5):723–734. <https://doi.org/10.1007/BF02703148>
- Saito H, Bellan MF, Al-Habshi A, Aizpuru M, Blasco F (2003) Mangrove research and coastal ecosystem studies with SPOT-4 HRVIR and TERRA ASTER in the Arabian Gulf. *Int J Remote Sens* 24(21):4073–4092. <https://doi.org/10.1080/0143116021000035030>
- Samara F, Solovieva N, Ghalayini T, Nasrallah ZA, Saburova M (2020) Assessment of the environmental status of the mangrove ecosystem in the United Arab Emirates. *Water*. 12(6):1623. <https://doi.org/10.3390/w12061623>
- Schwartz MD (2003) *Phenology: an integrative environmental science*. Kluwer Academic Publishers, Dordrecht
- Simard M, Fatoyinbo L, Smetanka C, Rivera-Monroy VH, Castañeda-Moya E, Thomas N, Van der Stocken T (2019) Mangrove canopy height globally related to precipitation, temperature and cyclone frequency. *Nat Geosci* 12:40–45
- Son NT, Thanh BX, Da CT (2016) Monitoring mangrove forest changes from multi-temporal Landsat data in Can Gio Biosphere Reserve, Vietnam. *Wetlands* 36(3):565–576. <https://doi.org/10.1007/s13157-016-0767-2>
- Srikanth S, Lum SK, Chen Z (2016) Mangrove root: adaptations and ecological importance. *Trees*. 30:451–465
- Su Mon M, Mizoue N, Htun NZ, Kajisa T, Yoshida S (2012) Estimating forest canopy density of tropical mixed deciduous vegetation using Landsat data: a comparison of three classification approaches. *Int J Remote Sens* 33(4):1042–1057. <https://doi.org/10.1080/01431161.2010.549851>
- Switzer AD, Yu F, Gouramanis C, Soria JLA, Pham DT (2014) Integrating different records to assess coastal hazards at multi-century timescales. *J Coas Res* 70:723–729. <https://doi.org/10.2112/SI70-122.1>
- Teixeira Pinto C, Jing X, Leigh L (2020) Evaluation analysis of Landsat level-1 and level-2 data products using in situ measurements. *Remote Sens* 12(16):2597
- Thakur S, Mondal I, Ghosh PB, Das P, De TK (2020) A review of the application of multispectral remote sensing in the study of mangrove ecosystems with special emphasis on image processing techniques. *Spat Inf Res* 28:39–51
- Townshend JR, Justice CO (1986) Analysis of the dynamics of African vegetation using the normalized difference vegetation index. *Int J Remote Sens* 7(11):1435–1445. <https://doi.org/10.1080/01431168608948946>
- Tran TV, Reef R, Zhu X (2022) A review of spectral indices for mangrove remote sensing. *Remote Sens* 14:4868. <https://doi.org/10.3390/rs14194868>
- Wang L, Jia M, Yin D, Tian J (2019) A review of remote sensing for mangrove forests: 1956-2018. *Remote Sens Environ* 231:111223. <https://doi.org/10.1016/j.rse.2019.111223>
- Zhang X, Treitz PM, Chen D, Quan C, Shi L, Li X (2017) Mapping mangrove forests using multi-tidal remotely-sensed data and a decision-tree-based procedure. *Int J Appl Earth Obs Geoinf* 62:201–214. <https://doi.org/10.1016/j.jag.2017.06.010>

Springer Nature or its licensor (e.g. a society or other partner) holds exclusive rights to this article under a publishing agreement with the author(s) or other rightsholder(s); author self-archiving of the accepted manuscript version of this article is solely governed by the terms of such publishing agreement and applicable law.